Magnetic Resonance Imaging 61 (2019) 73–82

Contents lists available at ScienceDirect

Magnetic Resonance Imaging

journal homepage: www.elsevier.com/locate/mri

Original contribution

Precision, reproducibility and applicability of an undersampled multi-venc 4D flow MRI sequence for the assessment of cardiac hemodynamics

Richard Moersdorf[a], Melanie Treutlein[a], Jan Robert Kroeger[a], Bram Ruijsink[b], James Wong[b], David Maintz[a], Kilian Weiss[a,c], Alexander C. Bunck[a], Bettina Baeßler[a], Daniel Giese[a,*]

[a] Department of Radiology, University of Cologne, Faculty of Medicine and University Hospital Cologne, Cologne, Germany.
[b] School of Biomedical Engineering and Imaging Sciences, King's College London, London, United Kingdom
[c] Philips GmbH, Hamburg, Germany

ARTICLE INFO

Keywords:
4D flow MRI
Multi-venc
k-t PCA
Blood flow quantification

ABSTRACT

Background and purpose: For the assessment of cardiovascular blood flow, 2D flow (2D) and 4D flow with a single venc (4D Mono) are established techniques. The objective of this study was to validate a multi-venc 4D flow (4D Multi) sequence for the improved simultaneous assessment of arterial and venous flow in high and low flow conditions and to investigate the scan-rescan reproducibility and inter-observer variability of the novel sequence.

Methods: Eleven volunteers with no known heart condition (female: 6, mean age: 25.8 ± 9.1 years) and two patients with a Fontan circulation were examined using phase-contrast 2D and 4D flow MRI. Stroke volumes, maximum velocities, net flow curves and internal consistency were measured and compared between 2D, 4D Mono and 4D Multi. Additionally, scan-rescan and inter-observer variabilities were analyzed. Finally, qualitative visualization comparisons were performed.

Results: Bland-Altman analysis show a higher agreement in stroke volumes between 4D Multi and 2D (7 ± 11%) than 4D Mono and 2D (11 ± 24%). 4D Multi is more accurate than 4D Mono in measuring time-resolved net flow throughout the cardiac cycle and qualitative blood flow visualization of 4D Multi is more accurate in visualizing flow patterns revealing more details and less artifacts than 4D Mono. Scan-rescan reproducibility is higher in 4D Multi (−0.04 ± 4.5 ml) than 2D (2.1 ± 7.3 ml) and inter-observer variability is low in both techniques (2D: −0.4 ± 3.4 ml and 4D Multi: 0.4 ± 3.5 ml). Internal consistency was improved in volunteers and patients when using 4D Multi as compared to 4D Mono.

Conclusion: 4D Multi offers a comprehensive way to accurately quantify flow in arteries and veins both in high and low flow situations and to visualize detailed flow patterns. This technique is readily applicable in the clinical setting and has the potential to be beneficial in the clinical assessment of valvular and congenital heart diseases.

1. Introduction

Time-resolved phase-contrast cardiovascular magnetic resonance in a two-dimensional slice using a single through-plane velocity encoding (venc) value (2D flow) is a well-established technique to quantify blood flow [1–3]. 2D flow has been compared to echocardiography [4,5], cardiac catheterization [6], radionuclide angiography [7] and invasive oximetry [8] leading to its acceptance and use in clinical cardiac MRI examinations [3]. To assess the flow through a specific vessel throughout the cardiac cycle a 2D slice has to be planned perpendicular to the vessel and is therewith highly dependent on operator skill and cardiovascular morphology [9,10]. Especially in patients with valvular or congenital heart diseases the placement of 2D slices remains cumbersome and challenging, leading to repeated scans and prolonged total examination times.

In recent years, time resolved phase-contrast MRI with three-dimensional spatial encoding and three-directional velocity encoding (4D flow) has been introduced. 4D flow enables full volumetric coverage of an anatomical volume of interest e.g. the heart and great vessels [11,12]. Using 4D flow, complex blood flow patterns can be visualized qualitatively and a retrospective quantification of velocities in arbitrarily placed 2D planes is possible. Furthermore, the planning of a 4D flow scan by placing a 3D volume of interest is quicker and more operator independent than planning several 2D slices during the

* Corresponding author at: Department of Radiology, University of Cologne, Kerpenerstr. 62, 50937 Cologne, Germany.
E-mail address: daniel.giese@uk-koeln.de (D. Giese).

https://doi.org/10.1016/j.mri.2019.05.015
Received 1 September 2018; Received in revised form 5 March 2019; Accepted 6 May 2019

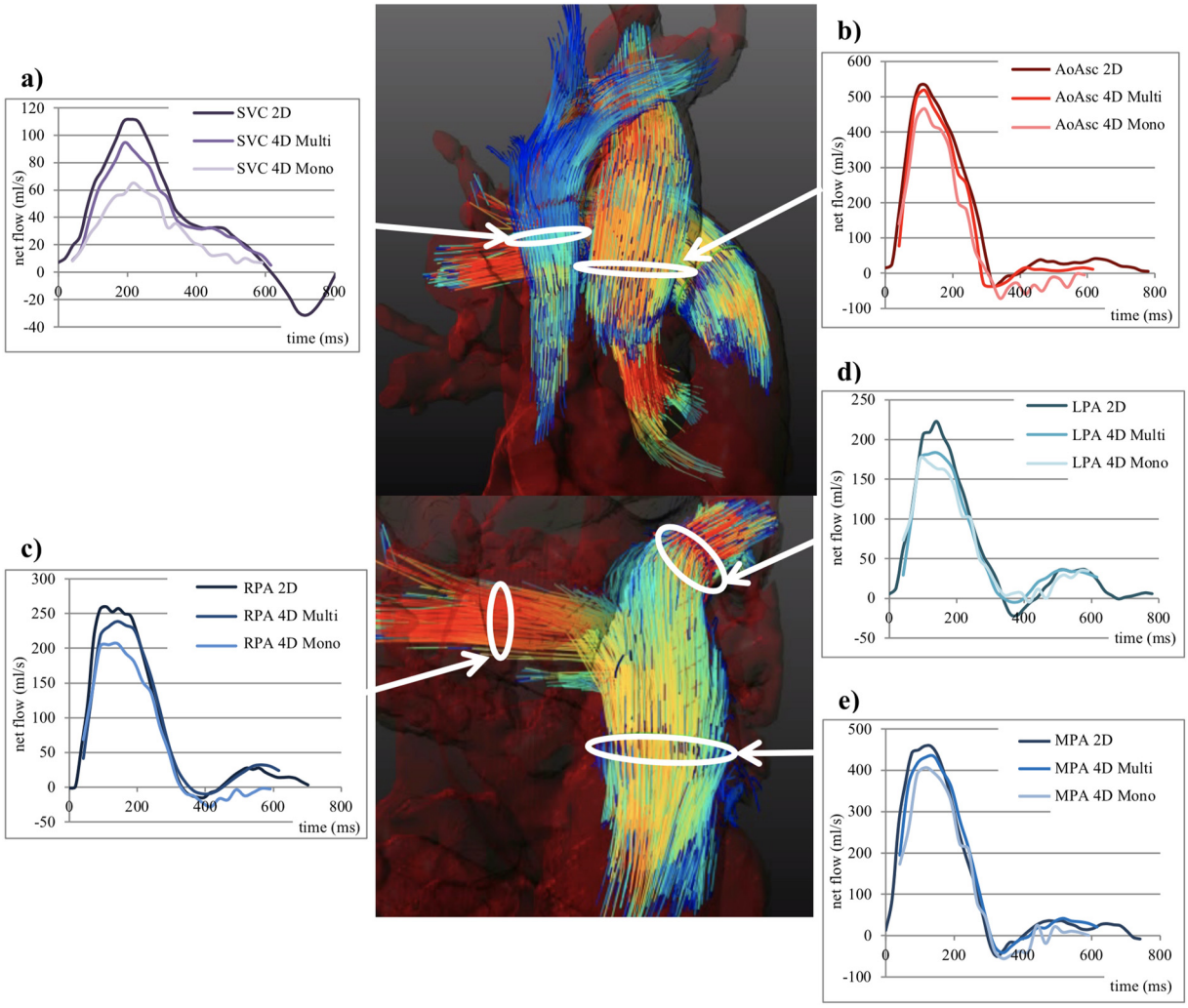

Fig. 1. Blood flow quantification was performed in 5 vessels: the ascending aorta (b), the main pulmonary artery (e), the left pulmonary artery (d), the right pulmonary artery (c) and the superior vena cava (a). Exemplary flow curves extracted from the 2D flow, the 4D Mono and the 4D Multi datasets are shown for each vessel.

acquisition. The main limitations of 4D flow however remain the long scan times, an elaborate data postprocessing with specifically designed software and the limited precision (i.e. lower velocity to noise ratios (VNR)) for velocities lower than the adjusted venc value [13]. Different undersampling techniques (*k-t* SENSE, *k-t* GRAPPA, *k-t* PCA) have helped reduce scan time to a feasible duration for clinical applications [14–16].

Most 4D flow studies use a single venc and mainly focus on arterial flow [9,17] and high flow situations (e.g. accelerated blood flow through valves) [18]. To prevent aliasing, the venc must be set above the expected maximum velocity. In a clinical setting, this maximum velocity can reach comparably high values of over 500 cm/s in stenoses, for instance. As the VNR is proportional to the measured velocity and inversely proportional to the venc, comparably lower velocities are measured with reduced accuracy [14,19,20]. These comparably lower velocities can occur during specific time-frames (e.g. during diastole in the aorta) and in regions of interest with generally smaller velocities (intra-cardiac or venous flow).

The approach of acquiring multiple venc values in a single scan with subsequent unaliasing of velocity data has been introduced [20–22] to overcome this issue. To allow for the longer scan times, sacrifices in geometrical coverage, spatio-temporal resolution or breathing motion artefacts are however often made.

Several studies have validated 4D flow measurements by comparison with 2D flow as a reference standard [14,17,23–25]. A few studies assessed the scan-rescan reproducibility and inter-observer variability in data analysis of 4D flow in specific anatomical regions e.g. thoracic [26] or abdominal aorta and renal arteries [27].

By combining *k-t* PCA [14] and Multi-venc 4D flow, the present study demonstrates the feasibility to accurately measure a larger range of velocities in the heart and great vessels as compared to a 4D flow acquisition with a single venc, in a clinical feasible scan time. The technique (4D Multi) is shown to enable more accurate simultaneous measurements of high and low flow conditions as compared to a single venc 4D flow approach (4D Mono). In healthy volunteers and focusing on five vessels of interest, haemodynamic parameters from 4D Multi are compared to 4D Mono and 2D flow acquisitions. To investigate scan-rescan reproducibility 2D and 4D scans were repeated shortly following each other. Inter-observer variability in data analysis was analyzed by comparing the results of two blinded observers. Finally, to show the techniques feasibility in a clinical routine setting, two patients with congenital heart defects (CHD) and Fontan circulation were acquired and flow data analyzed.

2. Materials and methods

2.1. Study population/subjects

The initial study was conducted in eleven volunteers with no known heart condition (female: 6, mean age: 25.8 ± 9.1 years). Furthermore, two patients with a Fontan circulation were acquired by adding the sequence to a clinically indicated MRI examination. Patient #1 was born with a hypoplastic left heart variant and underwent the Norwood, the Glenn and finally the Fontan procedure. Patient #2 had a tricuspid atresia and similarly underwent all stages to a final fenestrated Fontan circulation. The institutional ethics committees approved all acquisitions in our study and written informed consent was obtained from all participants.

2.2. MR imaging techniques

2.2.1. Volunteers

The volunteer study was conducted on a whole-body 3T MR scanner (Ingenia, Philips Healthcare, Best, The Netherlands, SW Ver: R5.3) using a 28-channel posterior and anterior matrix coil. The study protocol consisted of at least one set of five 2D flow and one 4D Multi scan. In eight out of eleven volunteers this set was repeated within the same scan session to investigate scan-rescan reproducibility, when the first set of scans didn't take longer than 60 min and the volunteer was willing and comfortable enough to undergo a second set of scans. All volunteers underwent the examination during a period of 60–120 min and all data, including the second scan set, were acquired within the same examination.

2D flow scans were performed in five different vessels: 1. ascending aorta (AoAsc) distal to the coronaries at the level of the main pulmonary artery; 2. main pulmonary artery (MPA) between valve and branching; 3. left pulmonary artery (LPA); 4. right pulmonary artery (RPA) 5. superior vena cava (SVC) 3–5 cm above the right atrium (Fig. 1). Plane planning was performed on a survey scan and three inflow weighted time-resolved gradient-echo scans acquired during free-breathing. 2D planes were positioned perpendicular to each vessel of interest. The venc was different for each vessel acquisition however remained fixed for all healthy volunteers. For the AoAsc and the MPA: 200 cm/s, for the LPA and RPA: 150 cm/s and for the SVC: 80 cm/s. Average nominal 2D flow scan durations were 13–24 s. 2D flow scans were performed with a respiratory navigator and a gating window of 5 mm resulting in a gating efficiency of approximately 60%. The scan quality was checked for velocity aliasing, incorrect anatomical positioning or poor angulation within the scan session and repeated when necessary. Additional acquisition parameters are listed in Table 1.

4D Multi scans were planned covering a sagittal 3D volume of the heart and the large thoracic vessels from the apex to the aortic arch in feet-head (FH) direction, anterior to posterior thorax wall in anterior-posterior (AP) [28] direction and SVC to the LPA branching in right-left (RL) direction. Three venc values were fixed to 200, 100 and 50 cm/s. Asymmetric encoding was performed leading to the acquisition of 1 flow-compensated image and 9 flow-encoded images (3 per spatial direction). These 10 images were nested in a 'beat-interleaved' way, leading to the acquisition of one segment of *k*-space of one image type per heart-beat. Scan acceleration was performed using a partial-Fourier factor of 0.75 and *k-t* undersampling on a sheared-grid pattern with an acceleration factor of 8 (number of training profile: 11 and 7 in k_y and k_z respectively). 4D Multi scans were performed with a respiratory navigator and a gating window of 5 mm resulting in a gating efficiency of 35%–60% (mean 47%). Retrospective cardiac triggering was performed with an arrhythmia rejection of heart cycles with lengths 5% over and 30% under the entered heart cycle lengths. Although the acquisition was performed using retrospective gating, the reconstruction (see below) was performed by neglecting data acquired after the 24th heart phase. Additional sequence parameters are shown in Table 1.

Table 1
Scan parameters.

	2D flow	4D Multi
Resolution (mm^3)	0.87–1.04 × 0.87–1.04 × 8	2.5 × 2.5 × 2.5
Field of view (mm^3)	AoAsc: 248 × 247 × 8 MPA: 258 × 358 × 8 LPA: 256 × 355 × 8 RPA: 250 × 300 × 8 SVC: 250 × 250 × 8	245.02 × 302.84 × 94.09
TE/TR (ms)	2.5/4.2	2.9/4.1
Flip angle (°)	10	8
Cardiac gating	Retrospective	Retrospective
Respiratory navigator window (mm)	5	5
Acquired heart phases	40	24
Scan time (nominal/net)	20/40 s	6.03/19.26 min
Number of VENC values	1	3
VENC values (cm/s) AoAsc/MPA/LPA/RPA/SVC	200/200/150/150/80	200, 100, 50

2.2.2. Patients

Patient datasets were acquired on a whole-body 1.5T MR scanner (Achieva, Philips Healthcare, Best, The Netherlands, SW Ver: R3.2). 4D Multi acquisition with the parameters described above were acquired following a clinically indicated cardiac MR acquisition.

2.3. Reconstruction and postprocessing

Reconstruction was performed offline using home-build algorithms in Matlab (Natick, USA) and was built upon ReconFrame (Gyrotool, Winterthur, Switzerland). Each encoded volume of the 4D flow data was reconstructed offline using *k-t* principal component analysis (*k-t* PCA) [14]. 4D Mono datasets were generated by extracting the data with a venc of 200 cm/s from the 4D Multi acquisition. 4D Multi data was generated using a model-based Bayesian velocity unfolding algorithm [29]. Total offline reconstruction times were in the order of 5 min per dataset on a workstation with 32 CPUs and 128GB of RAM. All datasets underwent concomitant field correction [30] as well as eddy-current background phase corrections using a second order polynomial fitting approach [31].

2D and 4D flow data were analyzed using GT Flow (Gyrotools, Winterthur, Switzerland, SW Ver: 3.0.20). 2D flow was quantified by manually drawing contours on each 2D image plane and adapted for every heart phase. Contours were drawn to include the vessel lumen while excluding the vessel wall. The 4D Mono and 4D Multi datasets were reformatted in planes at the corresponding geometry of the 2D flow data. Contours drawn on the 2D flow data were loaded into the 4D data and checked for correct positioning. Geometric contour mismatches due to different breathing positions between 4D and 2D flow were manually corrected.

2.4. Flow quantification

Stroke volumes (SV) in ml and time-resolved net flow volumes in ml/s were quantified in all five vessels of interest in volunteers on 2D flow, 4D Mono and 4D Multi. Furthermore, maximal velocity (v_{max}) in cm/s was quantified in all volunteers in the ascending aorta (AoAsc) as well as the pulmonary trunk (MPA) on 2D flow, 4D Mono and 4D Multi.

To investigate internal consistency based on mass conservation, the lossless connection between MPA and its two branches RPA and LPA ($Q_{MPA}/Q_{LPA+RPA}$) and the assessed pulmonary to systemic flow (Q_{MPA}/Q_{AoAsc}) ratios were calculated for 2D flow, 4D Mono and 4D Multi.

Inter-observer variability was analyzed by comparing SV through all five contours drawn by two independent observers on all datasets. Since

4D Multi and 4D Mono have identical geometries, inter-observer variability was performed on the 2D flow and 4D Multi datasets.

2.5. Statistical analysis

All data are expressed as mean ± standard deviation. The data range is shown by providing the minimum and maximum [min/max] values. Bland-Altman tests with limits of agreements (mean ± 1.96 * standard deviation) were performed to analyze:

- the difference between acquisition techniques, i.e. 2D vs. 4D Multi and 2D vs. 4D Mono
- the scan-rescan variations, i.e. 1 2D vs. 2 2D, 1 4D Multi vs. 2 4D Multi
- the inter-observer variabilities

To quantify conservation-of-mass, box plots were used.

A Pearson's correlation analysis including *p*-value and confidence interval assessments were also performed.

From the time-resolved net flow volume curves, two specific time periods, namely the “peak systolic flow” (PS) and the “peak retrograde flow” (PR) were defined on AoAsc and MPA flow curves. PS corresponds to the mean flow during the three heart-phases with the highest flow. PR corresponds to the mean flow during the three end-systolic heart-phases with the lowest flow (Fig. 2). In case of an incompetent valve, this is the period where retrograde flow would occur. The periods were defined for each subject and both vessels individually. To match the number of heart phases between the 2D flow (40 heart phases) and the 4D acquisitions (24 heart phases), 2D flow curves were down-sampled to 24 heart phases. For each subject and vessel mean volume flows in ml/s were calculated for 2D, 4D Multi and 4D Mono for PS and PR. The PS and PR deviations between 2D and 4D Multi and between 2D and 4D Mono are presented as box plots.

2.6. Qualitative flow visualization

GT Flow was also used to visualize and qualitatively compare 4D Multi and 4D Mono data. For better anatomical understanding, a velocity-weighted magnitude segmentation threshold was used. After drawing the previously described contours for each investigated vessel, particles were released and traced forward and backward in time (release interval: 11.6 ms, visual trace length: 11.6 ms). Quality features included the requirement for particles to stay within the blood pool of the vessel [23].

2.7. Patients

In both patients with Fontan circulation, an internal validation of flow volumes was performed. This mass conservation analysis is based on the following flow (Q) assumptions: $Q_{SVC} + Q_{IVC} = Q_{RPA} + Q_{LPA}$. In addition, a measure of particle statistics, proposed amongst other by [32] was also performed. This analysis counts the ratio of particles ejected from IVC or SVC arriving at RPA and LPA. Both internal flow validation and particle count analyses were performed on 4D Mono and 4D Multi. Finally, for visual comparison, movies of particles in the Fontan circulation were generated for both methods.

3. Results

The nominal scan time for the 4D Multi scan was 6.03 min (± 0.78 [5.18/7.48]) and the net scan time including breathing navigator efficiency and arrhythmia rejection was 19.26 min (± 5.76 [9.3/28.08]) in volunteers.

3.1. Quantitative analysis

Fig. 1 exemplary illustrates flow curves measured using 2D flow, 4D Mono and 4D Multi for all five vessels analyzed in one volunteer.

Fig. 3a presents Bland-Altman plots of SV measured using 2D flow as compared to 4D Mono and 4D Multi. In comparison to 2D flow, 4D Multi showed smaller differences in SV (7 ± 11% [−21/30%]) than 4D Mono (11 ± 24% [−91/62%]), especially in smaller arteries (LPA, RPA) and veins (SVC) with lower stroke volumes. Table 2 lists detailed values including mean deviations, standard deviations, ranges as well as the results of the Pearson's correlation analysis. 4D Multi shows higher correlation with 2D (correlation coefficient 0.974 $p < 0.01$) than 4D Mono (0.889 $p < 0.01$).

Fig. 3b shows the analysis of v_{max}. In comparison to 2D, 4D Multi showed smaller differences (0 ± 8% [−19/10%]) than 4D Mono (4 ± 12% [−23/27%]) and higher correlation with 2D (4D Multi 0.933 $p < 0.01$ vs. 4D Mono 0.832 $p < 0.01$ (Table 3).

Fig. 4 shows the results of the conservation-of-mass analysis. Especially for the MPA and RPA + LPA ($Q_{MPA}/Q_{LPA+RPA}$), improved internal consistency in 4D Multi (96 ± 5% [88/104%] is seen as

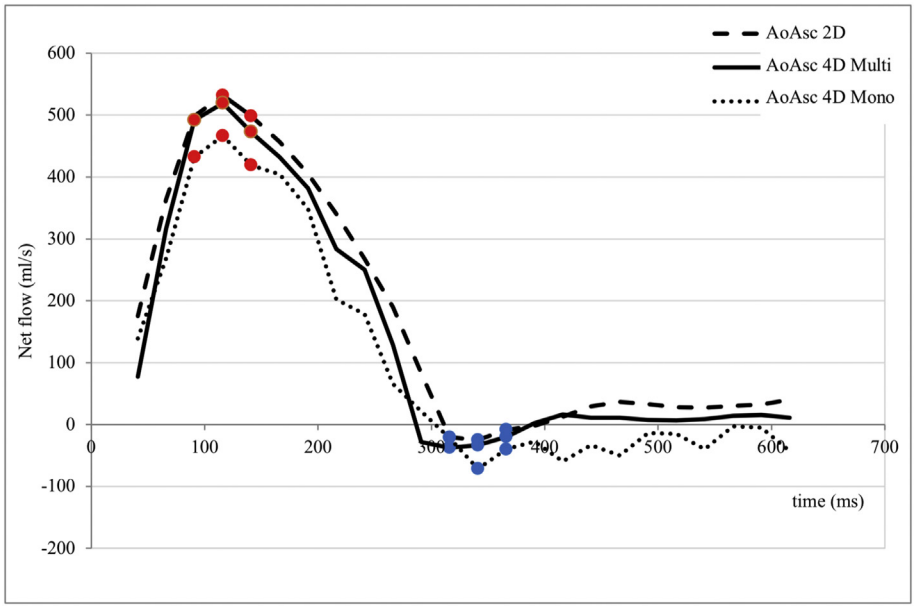

Fig. 2. Definition of the ‘peak systolic’ (PS) and ‘peak retrograde’ (PR) flow parameters shown exemplarily on net volume flow curves through the ascending aorta (2D flow, 4D Multi and 4D Mono). The mean flow during the 3 systolic (dark red) and the 3 end-systolic (dark blue) time points is calculated for the PS and PR quantification respectively. (For interpretation of the references to colour in this figure legend, the reader is referred to the web version of this article.)

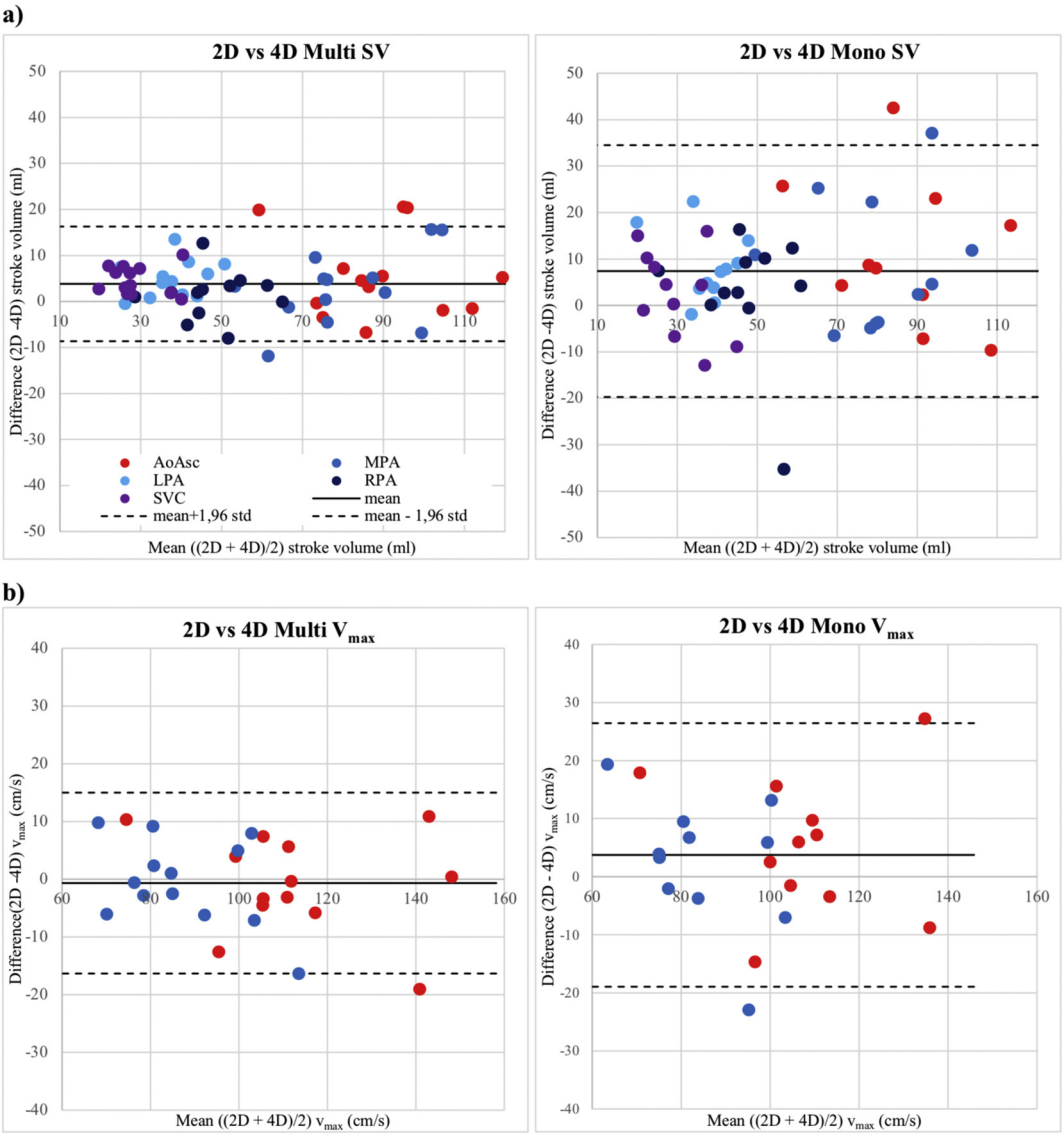

Fig. 3. Bland-Altman plots showing the differences in stroke volumes (a) and maximal velocity (b) between 2D and 4D Multi and 2D and 4D Mono.

Table 2
Differences in stroke volumes in percent as compared to 2D over all volunteers given in mean ± standard deviation [min/max] and Pearson's correlation coefficient (PCC) including 95% confidence interval values (CI).

	4D Mono	PCC (CI)	4D Multi	PCC (CI)
AoAsc	15.5 ± 19.0 [−9.4/46.8]	0.596 (−0.006/0.881)	5.9 ± 10.7 [−8.3/28.7]	0.8603* (0.538/0.963)
MPA	9.2 ± 16.0 [−9.9/32.9]	0.662 (0.103/0.903)	2.3 ± 9.9 [−21.5/14.2]	0.922* (0.722/0.980)
LPA	19.5 ± 19.9 [−5.9/61.9]	0.6152 (0.0242/0.888)	11.7 ± 9.2 [−2.1/29.8]	0.860* (0.539/0.963)
RPA	3.3 ± 32.9 [−90.8/30.3]	0.433 (−0.225/0.820)	2.0 ± 10.7 [−17.1/24.3]	0.874* (0.577/0.967)
SVC	7.7 ± 30.1 [−42.7/54.1]	0.539 (−0.089/0.8607)	14.9 ± 9.3 [1.1/29.6]	0.903* (0.661/0.975)
All vessels	11.1 ± 24.3 [−90.9/61.9]	0.889* (0.817/0.934)	7.5 ± 10.9 [−21.5/29.8]	0.974/* (0.956/0.985)

* $p < 0.01$.

compared to 4D Mono (100 ± 22% [49/135%]. The assessment of pulmonary to systemic flow (Q_{MPA}/Q_{AoAsc}) shows improved agreement in 4D Multi (92 ± 8% [84/105%] than in 4D Mono (95 ± 15% [70/127%].

Table 3
Differences in maximum velocities in percent as compared to 2D over all volunteers given in mean ± standard deviation [min/max] and Pearson's correlation coefficient (PCC) including 95% confidence interval values (CI).

	4D Mono	PCC (CI)	4D Multi	PCC (CI)
AoAsc	5.2 ± 12.2 [−14.7/27.13]	0.789* (0.359/0.943)	5.5 ± 9.3 [−19.1/10.8]	0.929* (0.744/0.982)
MPA	2.31 ± 11.3 [−23/19.3]	0.709 (0.191/0.918)	−0.5 ± 7.5 [−16.4/9.8]	0.795* (0.372/0.944)
Both vessels		0.832* (0.631/0.928)		0.933* (0.843/0.972)

* $p < 0.01$.

Finally, Fig. 5 shows results of flow quantification during both PS and PR. Higher agreement with 2D flow in the 4D Multi than 4D Mono both in the aorta and in the MPA is seen (median values): Aorta PS: 15.6 ml vs 58.8 ml; Aorta PR: −2.1 ml vs. 6.1 ml; MPA PS: 12.4 ml vs. 45.6 ml; MPA PR: −1.1 ml vs. -18.9 ml (Fig. 5).

3.2. Qualitative analysis

Flow visualization of both 4D Mono and 4D Multi data in all 5

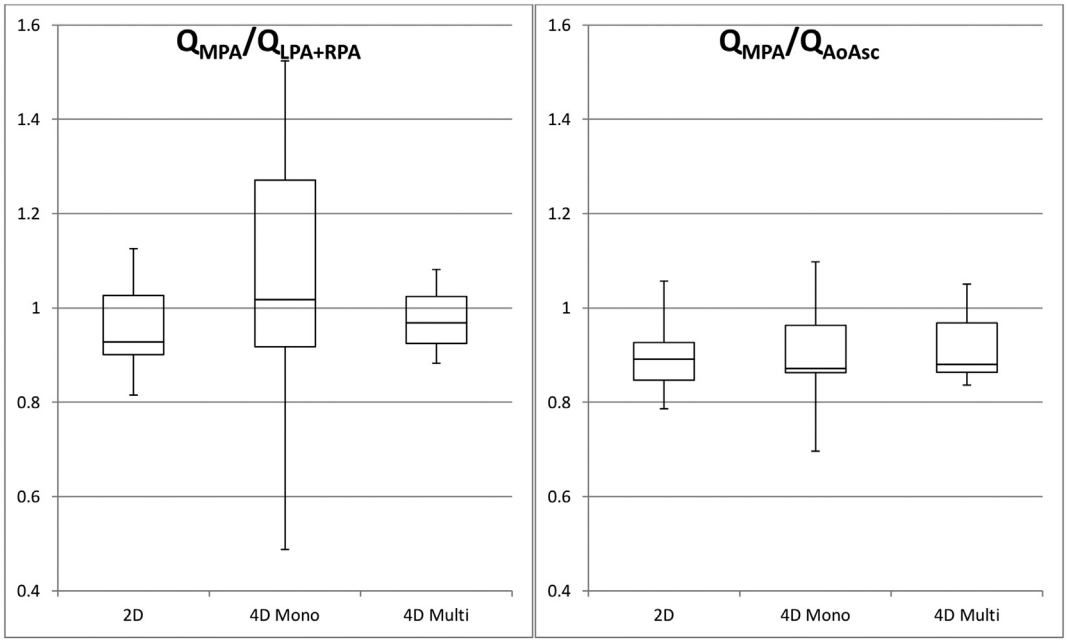

Fig. 4. Box plots showing conservation-of-mass analysis between MPA and LPA + RPA (left) and MPA and AoAsc (right).

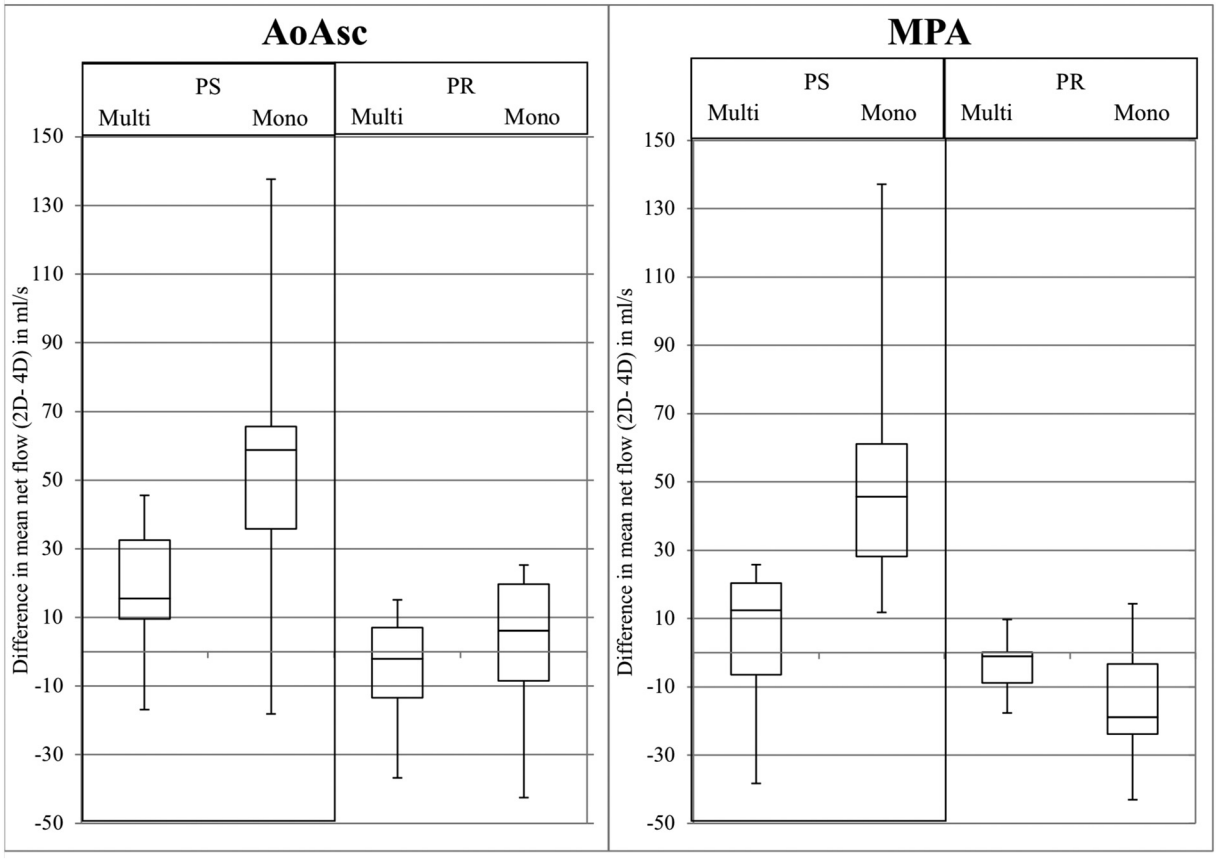

Fig. 5. Box plots showing averaged differences in peak systolic (PS) and peak retrograde (PR) flows in the ascending aorta and main pulmonary artery as compared to 2D flow.

vessels showed the expected flow patterns (e.g. aorta [33,34] and pulmonary arteries [35]). Examples are shown in Fig. 6. Corresponding movies are attached as additional files (Videos 1 to 6). When comparing 4D Mono to 4D Multi more particle traces remain inside the vessel lumen in the 4D Multi acquisition (e.g. Fig. 6A and E). For example, 4D Multi allows a better depiction of blood flow in the bifurcation of the right brachiocephalic artery (Fig. 6B), the vortex in the right atrium (Fig. 6D) or the branching of the right pulmonary artery (Fig. 6F).

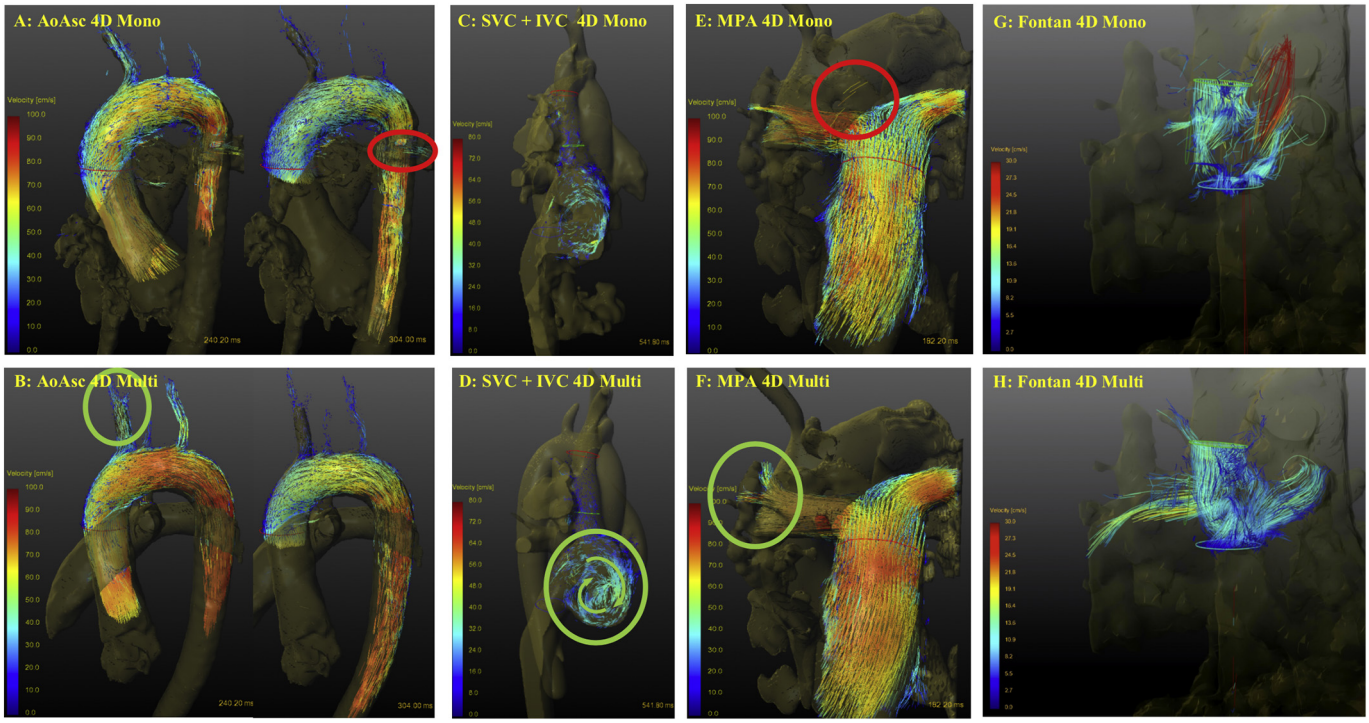

Fig. 6. 4D blood flow visualization using particle traces. 4D Mono (A, C, E, G) shows inaccurate flow pattern as compared to 4D Multi (B, D, F, H).

3.3. Scan-rescan reproducibility and inter-observer variability

Fig. 7 shows Bland-Altman plots of the scan-rescan and inter-observer variability analyses. 4D Multi showed better scan-rescan agreement (-0.04 ± 4.5 ml) than 2D (2.1 ± 7.3 ml). In both techniques, small vessels with lower SV (SVC, RPA, LPA) have a higher scan-rescan variability than larger vessels with higher velocities (AoAsc, MPA). Inter-observer variability is comparably low for both techniques (2D: -0.4 ± 3.4 ml and 4D: 0.4 ± 3.5 ml).

3.4. Patients

Table 4 shows the haemodynamic analysis of both patients in the Fontan circulation. The conservation-of-mass measurements as well as the particle count analysis are shown, performed on the 4D Multi and 4D Mono datasets. Movies of particle traces in both patients are provided as additional material (Videos 7–10) and a screenshot of data from patient #2 is given in Fig. 6G/H.

4. Discussion

The advantage of a 4D Multi acquisition covering the whole heart and great vessels is a time-efficient technique allowing the precise measurement of a large range of blood flow velocities in the cardiovascular system. This results in the ability to detect minor differences in flow volumes in both high and low flow conditions. Using an 8-fold spatio-temporal acceleration, 4D Multi acquisitions with 3 venc values covering the entire heart and surrounding vessels has herewith been shown feasible to be acquired in acceptable scan times with initial measurements in patients.

Quantitative flow measurements of 4D Multi showed good agreement with 2D flow measurements in-line with previous studies [9,17,36]. Remaining differences as compared to 2D flow can be attributed to several causes including physiological differences, temporal regularization in the *k-t* PCA reconstruction, flow encoding in a single direction in 2D flow and background phases in 2D and 4D flow. Rising gradient temperatures during long scans such as 4D Multi might further lead to unpredictable and varying background phase effects which are challenging to correct for [37].

In the aorta and pulmonary artery PS and small changes in PR can be measured with higher precision using 4D Multi as compared to 4D Mono. Especially in vessels with lower flow velocities throughout the cardiac cycle (e.g. SVC), measured flow values are closer to the reference standard 2D flow.

The assessment of the conservation-of-mass shows internal consistency in 4D Multi and the low distribution of values in comparison with 4D Mono indicates a higher precision in 4D Multi.

Scan-rescan analysis revealed good reproducibility and inter-observer variability showed a high observer independency of 4D Multi as compared to 2D flow. Possible reasons for lower scan-rescan reproducibility in 2D flow is the shorter scan-time and a possible change in heart rate between both 2D flow acquisition which would be averaged out in longer 4D Multi acquisitions.

4D Multi further showed improved qualitative assessment of blood flow not only in the great vessels but also intra-cardiac flow (e.g. vortex in the right atrium). Good visualization can for instance help to detect the site of the highest velocity within a stenotic jet and visually targeted quantification of this peak velocity is more reliable in estimating the stenosis severity than a 2D measurement [18].

4D Multi may help to understand the pathogenesis of cardiovascular diseases (e.g. aneurysm/dissection of the aorta, location of atherosclerotic plaques, thrombus formation) or to increase the diagnostic sensitivity of diseases with an altered blood flow like valvular or congenital heart diseases [11,15]. Application of the proposed 4D Multi in other thoracic vessels (inferior vena cava [36,38], pulmonary veins [39]) or anatomical regions (carotid arteries [40], intracerebral blood flow [41], intraabdominal flow in the portal vein [42], Truncus coeliacus) where studies have already applied 2D/4D flow techniques to investigate blood flow is of high interest.

The effect of the proposed 4D Multi acquisition and reconstruction of derived flow parameters such as wall shear stress [43], pressure gradients [44] or pulse wave velocities [45] has not been investigated in the current work. All of the above-mentioned parameters are however known to rely on high spatio-temporal resolution and good VNR.

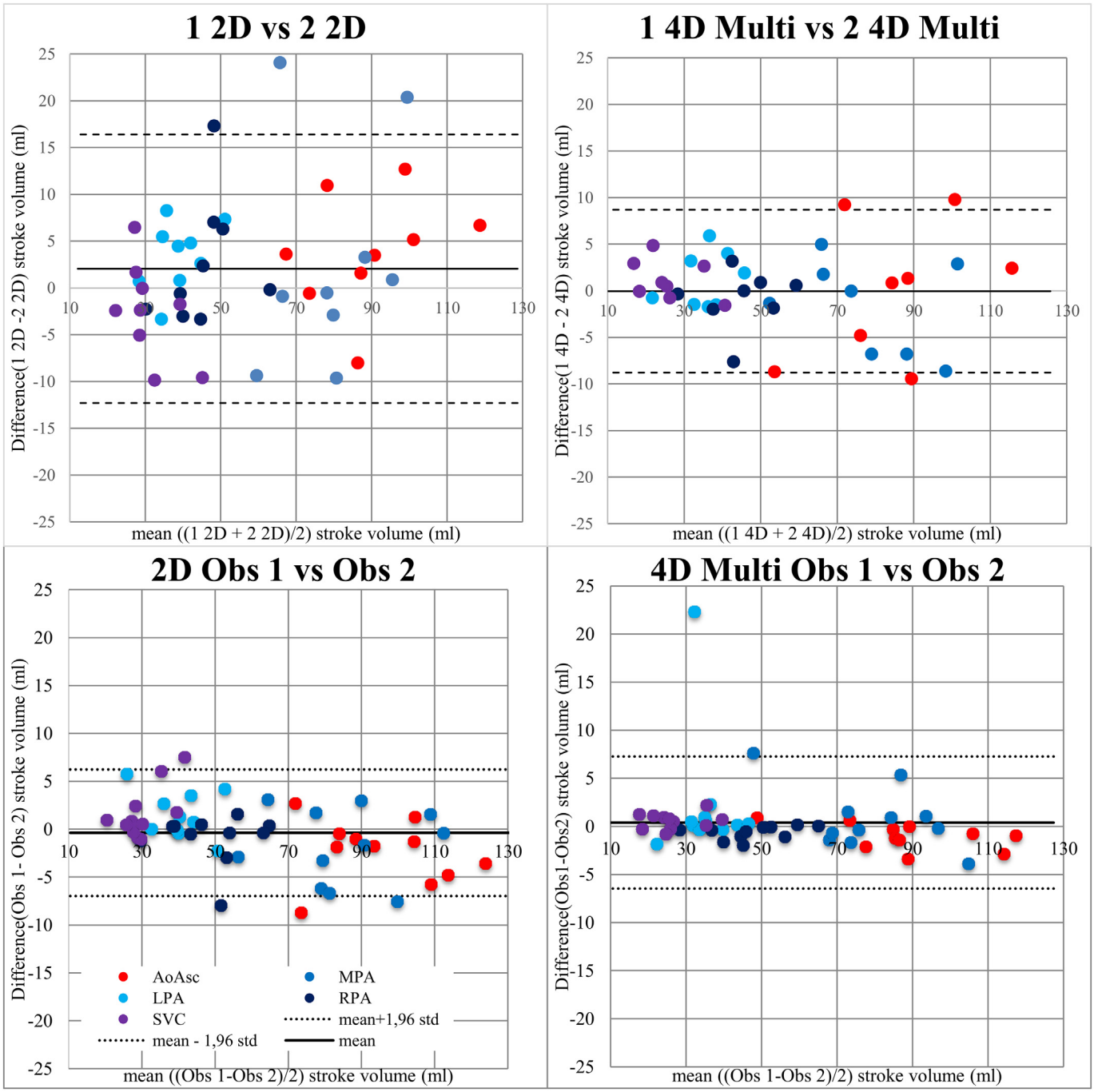

Fig. 7. Bland-Altman plots of scan-rescan reproducibility (upper row) and inter-observer variability (lower row) for stroke volumes measured in ml.

Table 4
Conservation-of-mass and particle count analysis in the Fontan circulation of both patients.

	Patient 1		Patient2	
	4D Mono	4D Multi	4D Mono	4D Multi
$(Q_{RPA} + Q_{LPA})/(Q_{IVC} + Q_{SVC})*100$	76%	87%	3%	108%
IVC➔RPA	13%	8%	100%	94%
SVC➔RPA	12%	71%	0%	16%

Using the proposed acceleration method could therewith be used to improve spatio-temporal resolution and VNR and potentially improve the calculation of advanced haemodynamic parameters. Finally, although the unfolding algorithm assumes a signal model which includes turbulent kinetic energy dissipation [29,46], its analysis would be beyond the scope of the current work.

Although neglecting breathing motion entirely when acquiring 4D flow is possible, we chose to comply with the consensus statement of navigator gating [12]. In combination with the *k-t* PCA sheared grid pattern, an optimized breathing-dependent k-space reordering scheme might allow to increase navigator efficiency and therewith reduce total scan time.

This is a study with a limited number of volunteers and patients. To further validate 4D Multi a larger study population is warranted. For the present 4D Multi, spatial and temporal resolution suggested in the consensus statement [12] were used. In comparison to 2D flow measurements the discrepancy in the temporal resolution (2D with 40 heart

phases and 4D with 24 heart-phases) might limit the significance of the current findings. The influence of different breathing patterns on the different techniques could also limit the comparability between 2D and 4D. Although a total scan duration for 4D Multi of approximately 20 min might be feasible in specific studies, a further reduction in scan time is desirable and could be achieved by applying new acceleration techniques in combination with non-cartesian sampling and optimizing respiratory gating. In the current study, a specific set of venc values was chosen: 50, 100 and 200 cm/s. Although a theoretical approach for the optimal choice of venc values has not been provided, we chose the largest venc value as the value that would be chosen for a single venc acquisition. The lowest venc was chosen in order to allow acceptably short echo times, in-line with the initial work of the Bayesian unfolding by Binter et al. [29]. The middle venc was chosen approximately in between both extreme values. For specific applications with very differing velocities (such as stenoses, coarctations, and others) a similar approach for the choice of the venc values is advised.

In conclusion, the present work demonstrates that 4D Multi in combination with *k-t* PCA acceleration improves flow quantification when compared to 4D Mono with *k-t* PCA. The acquisition of three venc values enabled a more precise measurement of a larger range of flow velocities both in high flow and low flow conditions (in space and time) in an acceptable scan time. Initial data in patients show that the sequence is readily integrated into clinical routine examinations of specific heart diseases.

Supplementary data to this article can be found online at https://doi.org/10.1016/j.mri.2019.05.015.

Funding

This research did not receive any specific grant from funding agencies in the public, commercial, or not-for-profit sectors.

Declaration of Competing Interest

Daniel Giese is employee of Siemens Healthcare since December 2018, all work related to this publication was performed prior or outside of his duties at Siemens.

References

[1] Pelc NJ, Herfkens RJ, Shimakawa A, Enzmann DR. Phase contrast cine magnetic resonance imaging. Magn Reson Q 1991;7(4):229–54.
[2] Underwood SR, Firmin DN, Klipstein RH, Rees RS, Longmore DB. Magnetic resonance velocity mapping: clinical application of a new technique. Br Heart J 1987;57(5):404–12.
[3] Lotz J, Meier C, Leppert A, Galanski M. Cardiovascular flow measurement with phase-contrast MR imaging: basic facts and implementation. Radiographics 2002;22(3):651–71.
[4] Caruthers SD, Lin SJ, Brown P, Watkins MP, Williams TA, Lehr KA, et al. Practical value of cardiac magnetic resonance imaging for clinical quantification of aortic valve stenosis: comparison with echocardiography. Circulation 2003;108(18):2236–43.
[5] Lin SJ, Brown PA, Watkins MP, Williams TA, Lehr KA, Liu W, et al. Quantification of stenotic mitral valve area with magnetic resonance imaging and comparison with Doppler ultrasound. J Am Coll Cardiol 2004;44(1):133–7.
[6] Hundley WG, Li HF, Willard JE, Landau C, Lange RA, Meshack BM, et al. Magnetic resonance imaging assessment of the severity of mitral regurgitation. Comparison with invasive techniques. Circulation 1995;92(5):1151–8.
[7] Arheden H, Holmqvist C, Thilen U, Hanseus K, Bjorkhem G, Pahlm O, et al. Left-to-right cardiac shunts: comparison of measurements obtained with MR velocity mapping and with radionuclide angiography. Radiology 1999;211(2):453–8.
[8] Petersen SE, Voigtlander T, Kreitner KF, Kalden P, Wittlinger T, Scharhag J, et al. Quantification of shunt volumes in congenital heart diseases using a breath-hold MR phase contrast technique–comparison with oximetry. Int J Cardiovasc Imaging 2002;18(1):53–60.
[9] Brix L, Ringgaard S, Rasmusson A, Sorensen TS, Kim WY. Three dimensional three component whole heart cardiovascular magnetic resonance velocity mapping: comparison of flow measurements from 3D and 2D acquisitions. J Cardiovasc Magn Reson 2009;11:3.
[10] Bollache E, van Ooij P, Powell A, Carr J, Markl M, Barker AJ. Comparison of 4D flow and 2D velocity-encoded phase contrast MRI sequences for the evaluation of aortic hemodynamics. Int J Cardiovasc Imaging 2016;32(10):1529–41.
[11] Markl M, Frydrychowicz A, Kozerke S, Hope M, Wieben O. 4D flow MRI. J Magn Reson Imaging 2012;36(5):1015–36.
[12] Dyverfeldt P, Bissell M, Barker AJ, Bolger AF, Carlhall CJ, Ebbers T, et al. 4D flow cardiovascular magnetic resonance consensus statement. J Cardiovasc Magn Reson 2015;17(1):72.
[13] Markl M, Kilner PJ, Ebbers T. Comprehensive 4D velocity mapping of the heart and great vessels by cardiovascular magnetic resonance. J Cardiovasc Magn Reson 2011;13(1):7.
[14] Giese D, Wong J, Greil GF, Buehrer M, Schaeffter T, Kozerke S. Towards highly accelerated Cartesian time-resolved 3D flow cardiovascular magnetic resonance in the clinical setting. J Cardiovasc Magn Reson 2014;16:42.
[15] Calkoen EE, Roest AA, van der Geest RJ, de Roos A, Westenberg JJ. Cardiovascular function and flow by 4-dimensional magnetic resonance imaging techniques: new applications. J Thorac Imaging 2014;29(3):185–96.
[16] Jung B, Ullmann P, Honal M, Bauer S, Hennig J, Markl M. Parallel MRI with extended and averaged GRAPPA kernels (PEAK-GRAPPA): optimized spatiotemporal dynamic imaging. J Magn Reson Imaging 2008;28(5):1226–32.
[17] Uribe S, Beerbaum P, Sorensen TS, Rasmusson A, Razavi R, Schaeffter T. Four-dimensional (4D) flow of the whole heart and great vessels using real-time respiratory self-gating. Magn Reson Med 2009;62(4):984–92.
[18] Nordmeyer S, Riesenkampff E, Messroghli D, Kropf S, Nordmeyer J, Berger F, et al. Four-dimensional velocity-encoded magnetic resonance imaging improves blood flow quantification in patients with complex accelerated flow. J Magn Reson Imaging 2013;37(1):208–16.
[19] Chai P, Mohiaddin R. How we perform cardiovascular magnetic resonance flow assessment using phase-contrast velocity mapping. J Cardiovasc Magn Reson 2005;7(4):705–16.
[20] Callaghan FM, Kozor R, Sherrah AG, Vallely M, Celermajer D, Figtree GA, et al. Use of multi-velocity encoding 4D flow MRI to improve quantification of flow patterns in the aorta. J Magn Reson Imaging 2016;43(2):352–63.
[21] Ha H, Kim GB, Kweon J, Kim YH, Kim N, Yang DH, et al. Multi-VENC acquisition of four-dimensional phase-contrast MRI to improve precision of velocity field measurement. Magn Reson Med 2016;75(5):1909–19.
[22] Nett EJ, Johnson KM, Frydrychowicz A, Del Rio AM, Schrauben E, Francois CJ, et al. Four-dimensional phase contrast MRI with accelerated dual velocity encoding. J Magn Reson Imaging 2012;35(6):1462–71.
[23] Carlsson M, Toger J, Kanski M, Bloch KM, Stahlberg F, Heiberg E, et al. Quantification and visualization of cardiovascular 4D velocity mapping accelerated with parallel imaging or k-t BLAST: head to head comparison and validation at 1.5 T and 3 T. J Cardiovasc Magn Reson 2011;13:55.
[24] Eriksson J, Carlhall CJ, Dyverfeldt P, Engvall J, Bolger AF, Ebbers T. Semi-automatic quantification of 4D left ventricular blood flow. J Cardiovasc Magn Reson 2010;12:9.
[25] Markl M, Chan FP, Alley MT, Wedding KL, Draney MT, Elkins CJ, et al. Time-resolved three-dimensional phase-contrast MRI. J Magn Reson Imaging 2003;17(4):499–506.
[26] Markl M, Wallis W, Harloff A. Reproducibility of flow and wall shear stress analysis using flow-sensitive four-dimensional MRI. J Magn Reson Imaging 2011;33(4):988–94.
[27] Wentland AL, Grist TM, Wieben O. Repeatability and internal consistency of abdominal 2D and 4D phase contrast MR flow measurements. Acad Radiol 2013;20(6):699–704.
[28] Ley S, Unterhinninghofen R, Ley-Zaporozhan J, Schenk JP, Kauczor HU, Szabo G. Validation of magnetic resonance phase-contrast flow measurements in the main pulmonary artery and aorta using perivascular ultrasound in a large animal model. Invest Radiol 2008;43(6):421–6.
[29] Binter C, Knobloch V, Manka R, Sigfridsson A, Kozerke S. Bayesian multipoint velocity encoding for concurrent flow and turbulence mapping. Magn Reson Med 2013;69(5):1337–45.
[30] Bernstein MA, Zhou XJ, Polzin JA, King KF, Ganin A, Pelc NJ, et al. Concomitant gradient terms in phase contrast MR: analysis and correction. Magn Reson Med 1998;39(2):300–8.
[31] Busch J, Giese D, Kozerke S. Image-based background phase error correction in 4D flow MRI revisited. J Magn Reson Imaging 2017;46(5):1516–25.
[32] Bachler P, Valverde I, Pinochet N, Nordmeyer S, Kuehne T, Crelier G, et al. Caval blood flow distribution in patients with Fontan circulation: quantification by using particle traces from 4D flow MR imaging. Radiology 2013;267(1):67–75.
[33] Morbiducci U, Ponzini R, Rizzo G, Cadioli M, Esposito A, Montevecchi FM, et al. Mechanistic insight into the physiological relevance of helical blood flow in the human aorta: an in vivo study. Biomech Model Mechanobiol 2011;10(3):339–55.
[34] Bogren HG, Buonocore MH. 4D magnetic resonance velocity mapping of blood flow patterns in the aorta in young vs. elderly normal subjects. J Magn Reson Imaging 1999;10(5):861–9.
[35] Barker AJ, Roldan-Alzate A, Entezari P, Shah SJ, Chesler NC, Wieben O, et al. Four-dimensional flow assessment of pulmonary artery flow and wall shear stress in adult pulmonary arterial hypertension: results from two institutions. Magn Reson Med 2015;73(5):1904–13.
[36] Valverde I, Nordmeyer S, Uribe S, Greil G, Berger F, Kuehne T, et al. Systemic-to-pulmonary collateral flow in patients with palliated univentricular heart physiology: measurement using cardiovascular magnetic resonance 4D velocity acquisition. J Cardiovasc Magn Reson 2012;14:25.
[37] Busch J, Vannesjo SJ, Barmet C, Pruessmann KP, Kozerke S. Analysis of temperature dependence of background phase errors in phase-contrast cardiovascular magnetic resonance. J Cardiovasc Magn Reson 2014;16:97.
[38] Nordmeyer S, Riesenkampff E, Crelier G, Khasheei A, Schnackenburg B, Berger F, et al. Flow-sensitive four-dimensional cine magnetic resonance imaging for offline

blood flow quantification in multiple vessels: a validation study. J Magn Reson Imaging 2010;32(3):677–83.
[39] Goo HW, Al-Otay A, Grosse-Wortmann L, Wu S, Macgowan CK, Yoo SJ. Phase-contrast magnetic resonance quantification of normal pulmonary venous return. J Magn Reson Imaging 2009;29(3):588–94.
[40] Kadbi M, Negahdar M, Traughber M, Martin P, Amini AA. Assessment of flow and hemodynamics in the carotid artery using a reduced TE 4D flow spiral phase-contrast MRI. Conf proc IEEE Eng med biol Soc, 2013. 2013. p. 1100–3.
[41] Schubert T, Bieri O, Pansini M, Stippich C, Santini F. Peak velocity measurements in tortuous arteries with phase contrast magnetic resonance imaging: the effect of multidirectional velocity encoding. Invest Radiol 2014;49(4):189–94.
[42] Nanashima A, Shibasaki S, Sakamoto I, Sueyoshi E, Sumida Y, Abo T, et al. Clinical evaluation of magnetic resonance imaging flowmetry of portal and hepatic veins in patients following hepatectomy. Liver Int 2006;26(5):587–94.
[43] Stalder AF, Russe MF, Frydrychowicz A, Bock J, Hennig J, Markl M. Quantitative 2D and 3D phase contrast MRI: optimized analysis of blood flow and vessel wall parameters. Magn Reson Med 2008;60(5):1218–31.
[44] Ebbers T, Wigström L, Bolger AF, Engvall J, Karlsson M. Estimation of relative cardiovascular pressures using time-resolved three-dimensional phase contrast MRI. Magn Reson Med 2001;45(5):872–9.
[45] Markl M, Wallis W, Brendecke S, Simon J, Frydrychowicz A, Harloff A. Estimation of global aortic pulse wave velocity by flow-sensitive 4D MRI. Magn Reson Med 2010;63(6):1575–82.
[46] Binter C, Gotschy A, Sundermann SH, Frank M, Tanner FC, Luscher TF, et al. Turbulent kinetic energy assessed by multipoint 4-dimensional flow magnetic resonance imaging provides additional information relative to echocardiography for the determination of aortic stenosis severity. Circ Cardiovasc Imaging 2017;10(6).